Development of the Gas Induced Semi-Solid Metal Process for Aluminum Die Casting Applications

J. Wannasin[1,a], S. Junudom[1,b], T. Rattanochaikul[1,c], M.C. Flemings[2,d]

[1]Department of Mining and Materials Engineering, Prince of Songkla University, Hat Yai, 90112,

Thailand

[2]Department of Materials Science and Engineering, Massachusetts Institute of Technology, Cambridge, MA, 02139, USA

[a]jessada.w@psu.ac.th, [b]r-somchai@hotmail.com, [c]r.tanate@yahoo.com, [d]flemings@mit.edu

Keywords: Gas Induced Semi-Solid; Rheocasting; Die Casting; Semi-Solid Metal; ADC10.

Abstract. A simple and efficient rheocasting process that has recently been invented is being developed for aluminum die casting applications. The process called Gas Induced Semi-Solid (GISS) utilizes the combination of local rapid heat extraction and agitation achieved by the injection of fine gas bubbles through a graphite diffuser to create semi-solid slurry. In the GISS process, the die casting machine and the process cycle remain little changed from those of conventional die casting. The GISS unit creates a low solid fraction of semi-solid slurry in the ladle during the ladle transfer to the shot sleeve. The semi-solid slurry is then poured directly into the shot sleeve. This paper presents the detailed description of the process. The results of the semi-solid die casting experiments with ADC10 alloy using the GISS process are also reported and discussed.

Introduction

Aluminum semi-solid components have been produced by thixocasting for many years. The process, however, has some cost disadvantages. For example, new equipment for cutting, reheating, and forming are often needed. Special aluminum billets used in the process also have higher costs than normal ingots used in conventional die casting. In addition, the scrap materials cannot be recycled in-house. These disadvantages result in use of semi-solid metal processing being limited to niche applications [1]. To widen the applications of semi-solid metal, research and development activities are focusing on rheocasting, which offers lower capital and materials costs. In a rheocasting processes, the die casting machine only requires minor modifications. In addition, normal aluminum ingots can be used for production and recycled in-house.

In the past five years, several rheocasting processes have been invented. Examples of the rheocasting processes are the NRC [2], SSR [3], CRP [4], Hitachi [5], SLC [6], and SEED [7] processes. However, some of these current rheocasting processes are still quite complex and expensive. A simple and efficient rheocasting process that has recently been invented is being developed for aluminum die casting applications. The process is called Gas Induced Semi-Solid (GISS). The mechanism of this process in forming semi-solid structure is the combination of local rapid heat extraction and agitation achieved by the injection of fine gas bubbles through a graphite diffuser to create semi-solid slurry [8-9]. This paper presents the detailed description of the process. The results of the semi-solid die casting experiments using the GISS process are also reported and discussed.

Experiments

The Gas Induced Semi-Solid (GISS) Process. The GISS process applies the knowledge that the semi-solid structure can be efficiently formed by the combination of local rapid heat extraction and agitation [10]. In the GISS process, the local rapid heat extraction occurs at the surfaces of the porous graphite diffuser when it is submerged in liquid aluminum. At the same time, vigorous agitation is induced at the chill surfaces by the flow of very fine inert gas bubbles out of the porous graphite. Figure 1 shows the schematic of the GISS process.

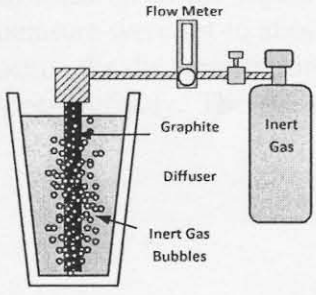

Fig. 1. Schematic of the Gas Induced Semi-Solid (GISS) process.

The GISS Die Casting Process. In the GISS die casting process, the die casting equipment and the process cycle remain little changed from those of conventional die casting. The only added step occurs during the ladle transfer when a graphite diffuser is immersed for about 10 seconds to create semi-solid slurry with a low solid fraction of about 10%. The semi-solid slurry is then poured into the shot sleeve for a die casting injection to produce a semi-solid casting part. Figure 2 shows the schematic of the GISS die casting process.

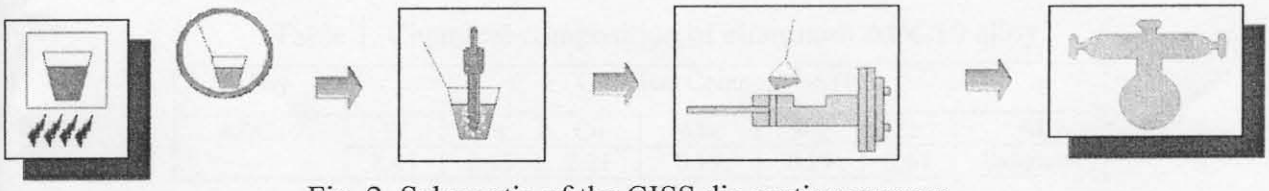

Fig. 2. Schematic of the GISS die casting process.

Laboratory Die Casting Machine. A laboratory-scale die casting machine with a 20-ton capacity was constructed for the development of the GISS die casting process. The medium-carbon steel die was used to produce tensile test rods with the diameter of 13 mm and the length of 130 mm. The dimensions and picture of the machine are given in Figure 3. Two gate diameters were used in this study: a thin gate with 2 mm thick and a thick gate with 6 mm thick. Figure 4 shows the thin and the thick gates used.

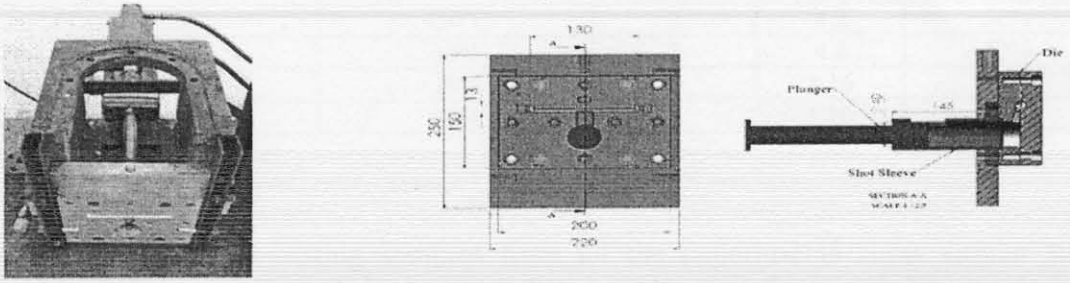

Fig. 3. The 20-ton laboratory die casting machine.

The GISS Die Casting Experiments with ADC10. Aluminum die casting alloy ADC10 (A380 equivalent) was used in this development. The chemical composition of this alloy is given in Table 1.

Experimental procedure. Aluminum ADC10 alloy was melted in a graphite crucible in an electric furnace. The metal was fluxed before casting. The ladle cup was made of stainless steel coated with boron nitride. Four sets of die casting experiments were conducted, including (1) Liquid Die Casting, (2) SSM-Thin Gate, (3) SSM-Thick Gate, and SSM-High Fill Fraction. A summary of the experimental conditions of the four sets is presented in Table 2. Other processing conditions are as follows. In the liquid die casting experiments, the die temperature and the shot sleeve temperature were set to about 150°C and 200°C, respectively. In the semi-solid die casting experiments, the die temperature and the shot sleeve temperature were set to about 300°C and 350°C, respectively. The plunger speed of all the experiments was about 0.12 m/s.

(a) (b)

Fig. 4. Drawings showing a 2-mm gate (a), and a 6-mm gate (b).

Table 1. Chemical composition of aluminum ADC10 alloy.

Alloy	Chemical Composition (%)						
ADC10	Si	Fe	Cu	Mn	Mg	Zn	Al
	8.47	0.95	2.21	0.19	0.29	0.61	Balanced

The die casting samples were then examined for surface defects. A tensile test was performed using about 5 samples for each experiment set. The macrostructure and microstructure were also studied using standard procedures.

Table 2. Summary of experimental conditions.

Experiment	Pouring Temperature or Solid Fraction in the Shot Sleeve	Gate Thickness (mm)	Gate Velocity (m/s)	Shot Sleeve Fill Fraction
1. Liquid Die Casting	650°C	2	4.2	50%
2. SSM-Thin Gate	10%	2	4.2	50%
3. SSM-Thick Gate	10%	6	1.16	50%
4. SSM-High Fill Fraction	10%	6	1.16	80%

Results and Discussion

Surface Finish. The die casting samples from all the experiments show similar surface quality. No differences can be observed between the casting samples produced by conventional liquid die casting and semi-solid die casting. Representative pictures showing the surface quality of the die casting samples are given in Figure 5.

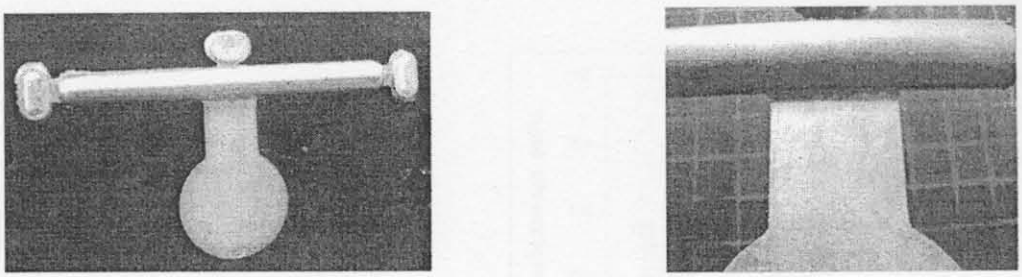

Fig. 5. Surface quality of representative die casting samples.

Macrostructure. Examination of the cross sections of the die casting samples for macroscopic defects showed two types of defects: air bubbles and shrinkage porosity. The Liquid Die Casting and SSM-Thin Gate samples had a lot of air bubbles inside (Figures 6a-6b). However, the SSM-Thick Gate and SSM-High Fill Fraction samples do not have any air bubbles inside (Figure 6d). Most samples have some shrinkage porosity near the gate (Figure 6c).

Analysis of the gate velocity shows that very high gate velocity, about 4.2 m/s, was obtained in the Liquid Die Casting and SSM-Thin Gate cases. In these cases, the flow of the metal into the die would be turbulent, resulting in trapped air bubbles. When the gate velocity was reduced to about 1.16 m/s by increasing of the gate thickness (the SSM-Thick Gate and SSM-High Fill Fraction cases), the flow of the metal changed to laminar. No trapped air bubbles were then observed in these samples.

The reason for some shrinkage porosity near the gate area might be because hot spots occurred near the gate area. In addition, the laboratory die casting machine did not have the capability to apply pressure intensification after the injection. Feeding during solidification might not be sufficient.

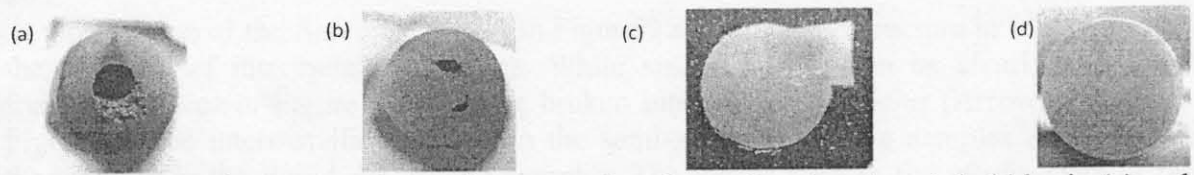

Fig. 6. Representative macro views of cross sectioned samples showing air bubbles in (a) and (b), shrinkage porosity in (c), and sound structure in (d).

Tensile Test. Two tensile specimens with the gauge length of 25 mm and diameter of 5 mm were machined from each casting rod, see Figure 7. A tensile test was then performed to determine the ultimate tensile strength (UTS) of the castings. The results are presented in Figure 8.

The UTS data of the Liquid Die Casting, SSM-Thin Gate, SSM-Thick Gate, and SSM-High Fill Fraction are 125±36, 144±32, 199±9, 213±8 MPa, respectively. Since the Liquid Die Casting and SSM-Thin Gate samples contained air bubbles, the UTS data are quite low. The standard deviation data are also quite large indicating the presence of air bubbles with various sizes in the castings. The fracture surfaces of the samples as shown in Figures 9a and 9b confirm that the low strengths are due to air bubbles.

When the castings were free from air bubble defects (SSM-Thick Gate and SSM-High Fill Fraction samples) as shown in Figures 9c and 9d, the UTS data are quite high and the standard deviation data are quite small. The limited number of data also suggests that a higher fill fraction of semi-solid slurry in the shot sleeve gives slightly better mechanical properties. Less waving flow of the slurry in the shot sleeve due to the higher level might be the reason for the improvement.

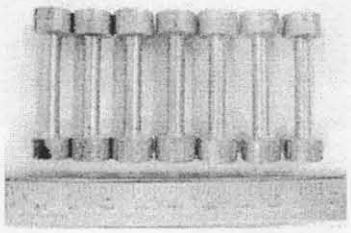

Fig. 7. Examples of the tensile test specimens.

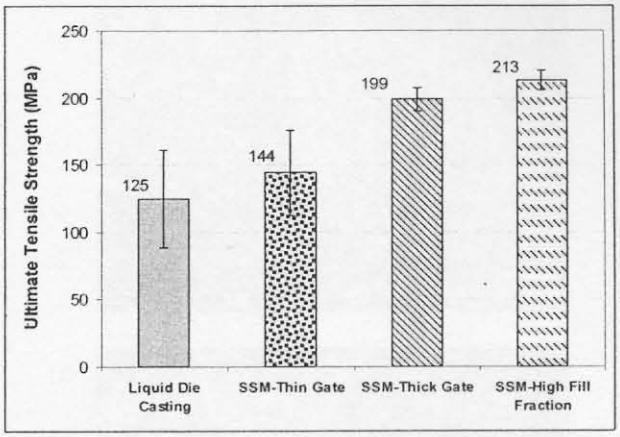

Fig. 8. Ultimate tensile strength of the samples.

Microstructure. Different microstructures are clearly observed in the four cases of experiments. As expected, dendritic microstructure is obtained in the Liquid Die Casting samples, Figure 10a. A mixture of coarse and fine equiaxed primary phase particles is obtained in the SSM-Thin Gate samples, Figure 10b. In this case, a small solid fraction of semi-solid metal was injected into the die at a high speed (4.2 m/s). The high shear and high cooling rate during the turbulent flow into the die resulted in the fine equiaxed particles. The high cooling rate also caused unstable growth of the pre-existing solid particles, which yielded non-globular structure of the semi-solid grains. With a lower speed and smoother flow into the die for the cases of SSM-Thick Gate and SSM-High Fill Fraction, the cooling rate of the semi-solid slurry was slower. With a slower cooling rate, the growth of the solid particles was more stable resulting in more globular structure as presented in Figures 10c and 10d.

Observation of the fracture surfaces in Figure 9 and the microstructure in Figure 10 shows the presence of intermetallic particles. White sparkling dots can be clearly seen on the fracture surfaces in Figure 9 indicating broken intermetallic particles (Arrows). As seen in Figure 11, the intermetallic particles in the semi-solid die casting samples are larger than those found in the liquid die casting samples. The longer time in the mushy state of these intermetallic particles in the semi-solid die casting allows the particle to grow to a larger size. These intermetallic particles are detrimental to the strength and ductility.

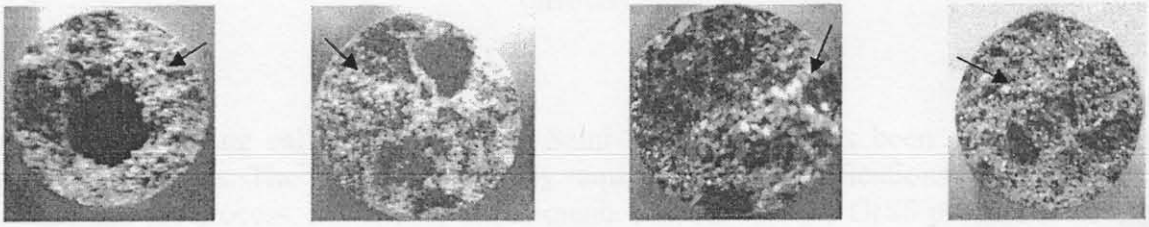

(a) Liquid Die Casting (b) SSM-Thin Gate (c) SSM-Thick Gate (d) SSM- High Fill Fraction

Fig. 9. Fracture surfaces of representative samples. Arrows point at intermetallic phases.

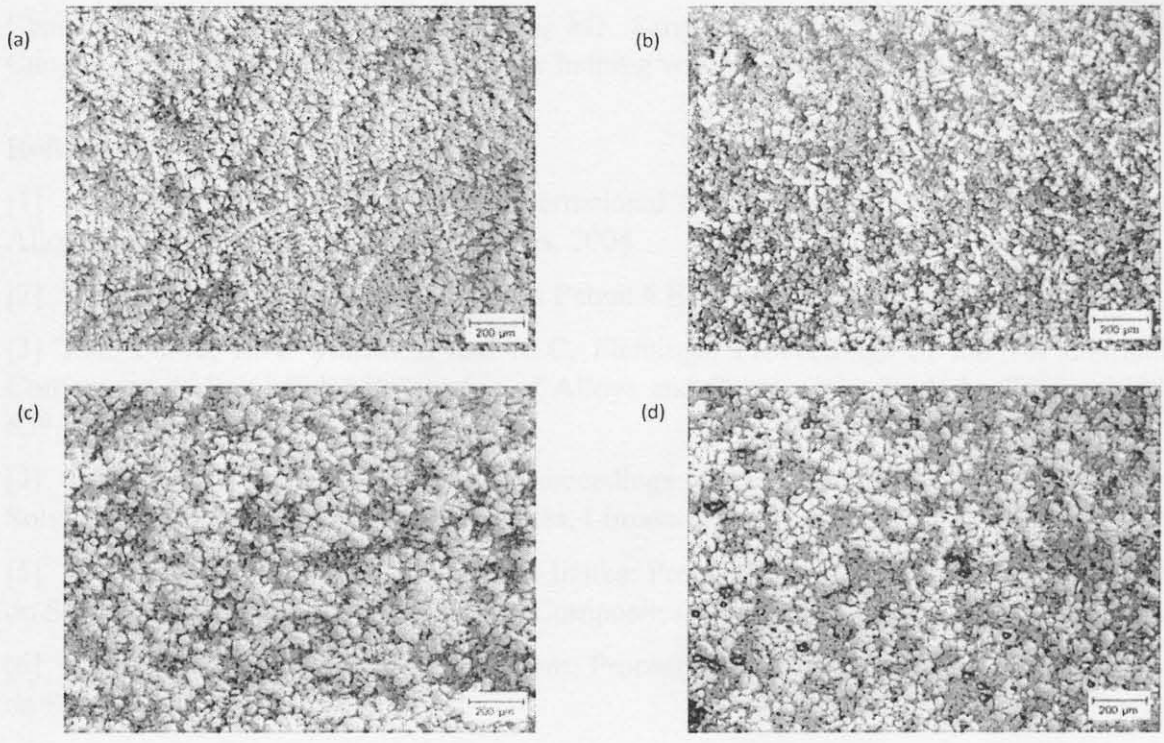

Fig. 10. Representative microstructures of the samples: (a) Liquid Die Casting, (b) SSM-Thin Gate, (c) SSM-Thick Gate, (d) SSM-High Fill Fraction.

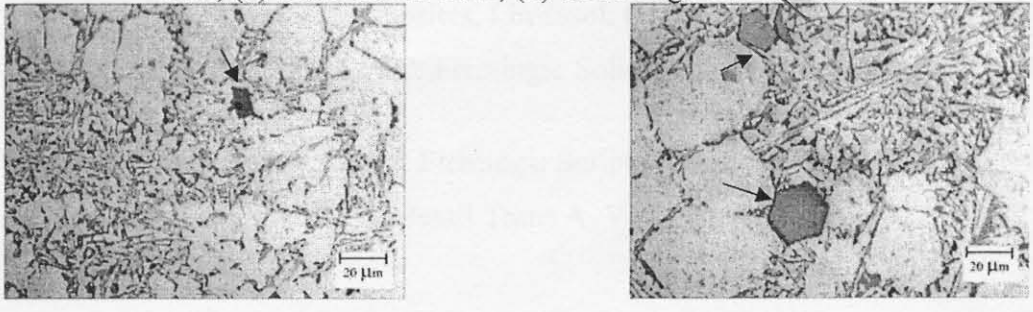

(a) Liquid Die Casting (2) Semi-Solid Die Casting

Fig. 11. Representative micrographs showing the eutectic and intermetallic phases (arrows).

Summary

The new rheocasting called Gas Induced Semi-Solid (GISS) has been developed for die casting applications. The GISS process only requires minor modifications to the die casting machine and the process. Laboratory experiments confirm that the GISS process can be used to produce castings with improved mechanical properties compared to conventional liquid die casting. Adjustments of the process parameters such as temperatures and plunger speeds and the gating system are required in order to achieve the sound casting parts.

Acknowledgements

The authors gratefully acknowledge the financial supports from the Reverse Brain Drain Project (RBD), the National Science and Technology Development Agency (NSTDA), and the Thai Research Fund (Contract No. MRG4980110). We also thank Mr. Suchart

Chantaramanee, Mr. Romadorn Burapa, Mr. Sangop Thanabumrungkul, Miss Rungsinee Canyook, and Miss Chutima Karakate for helping with the experiments.

References

[1] J.L. Jorstad: Proceedings of 8th International Conference on Semi-Solid Processing of Alloys and Composites, Limassol, Cyprus, 2004

[2] Ube Industries Ltd., Japan: European Patent # EP0 745 694 A1, Dec. 4, 1996

[3] J.A. Yurko, R.A. Martinez, and M.C. Flemings: Proceedings of the 7th International Conference on Semi-Solid Processing of Alloys and Composites, Tsukuba, Japan, 2002, pp. 659-664

[4] Q.Y. Pan, M. Findon, D. Apelian: Proceedings of 8th International Conference on Semi-Solid Processing of Alloys and Composites, Limassol, Cyprus, 2004

[5] R. Shibata, T. Kaneuchi, T. Soda, Y. Iizuka: Proceedings of 4th International Conference on Semi-Solid Processing of Alloys and Composites, Sheffield, England, 1996, pp. 296-300

[6] J. Jorstad, M. Thieman, and R. Kamm: Proceedings of the 7th International Conference on Semi-

Solid Processing of Alloys and Composites, Tsukuba, Japan, 2002, pp. 701-706

[7] D. Doutre, J. Langlais, S. Roy: Proceedings of 8th International Conference on Semi-Solid Processing of Alloys and Composites, Limassol, Cyprus, 2004

[8] J. Wannasin, R.A. Martinez, M.C. Flemings: Solid State Phenom. Vol. 116 (2006), pp. 366-369

[9] J. Wannasin, R.A. Martinez, M.C. Flemings: Scripta Mater. Vol. 55 (2006), pp. 115-118

[10] R.A. Martinez, M.C. Flemings: Metall Trans A. Vol. 36 (2005), pp. 2205-2210

Evaluation of Solid Fraction in a Rheocast Aluminum Die Casting Alloy by a Rapid Quenching Method

Jessada Wannasin[1,*], Rungsinee Canyook[1], Romadorn Burapa[1], Merton C. Flemings[2]

[1]*Department of Mining and Materials Engineering, Prince of Songkla University, Songkhla, Hat Yai, 90112, Thailand*

[2]*Department of Materials Science and Engineering, Massachusetts Institute of Technology, Cambridge, MA, 02139, USA*

Abstract

A new approach to evaluate the solid fraction of semi-solid slurries is reported. The approach applies a thin-channel vacuum mold to rapidly quench semi-solid slurries at different rheocasting times. The slurry temperatures are analyzed from the cooling curves. The corresponding solid fraction data are obtained from standard quantitative metallography. A correction of the data is then conducted using the average growth layer of the solid particles. The analyzed solid fraction agrees well with the data from the Scheil model.

Keywords: Semi-solid metal; Solid fraction; Rheocasting; Quenching method; Die casting

Semi-solid metal forming has been applied commercially on aluminum alloys for several years. Most of the applications have used Al-Si-Mg alloys such as A356 and A357 alloys because of the wide processing window for semi-solid forming and the high strength

* Corresponding author. Tel.: +66 74 212 897; e-mail: jessada.w@psu.ac.th

and ductility it offers [1]. Recently, semi-solid rheocasting processes have also been applied to Al-Si-Cu-Fe alloys such as A380 or ADC10 alloy to give process and quality improvements in die casting applications [2-3]. In a rheocasting process of these die casting alloys, instead of casting superheated liquid metal, semi-solid slurry with a low solid content of about 10 percents is poured into a shot sleeve [4]. The solid content then increases to a high fraction of about 40 to 60 percents by the time the semi-solid slurry enters the die. Faster process cycle time, longer die life, less lubricants used, and reduced rejected parts due to less porosity are some of the advantages of the semi-solid die casting process [1].

To efficiently apply this rheocasting process in die casting applications, it is important to have a reliable solid fraction curve and to control the morphology of the solid particles in the semi-solid slurry at the low fractions in order to control the flow behavior of the semi-solid metal in the die cavity. Several methods may be used to determine the evolution of solid fraction of metals. These methods discussed in detail by Tzimas and Zavaliangos [5] are utilization of thermodynamic data, quantitative metallography on microstructures quenched from the semi-solid state, thermal analysis techniques, ultrasonic monitoring, measurement of electrical resistance/magnetic permeability, and measurement of mechanical response. From these methods, only quantitative metallography on microstructures quenched from the semi-solid state is suitable for studying the evolution of the solid fraction of semi-solid slurry, because the technique also reveals the solid particle morphology.

Various quenching methods have been reported by several investigators such as by Tzimas and Zavaliangos [5], de Figueredo *et al.* [6], and Chen and Huang [7]. In these quenching methods, samples with medium to high solid fractions in the range of about 15% to 94% are reheated to the corresponding temperatures before quenching. The information of the microstructure evolution obtained by these quenching methods is useful for the controls of thixocasting processes [5]. However, these previous methods are not suitable to evaluate

the solid fraction and the particle morphology in rheocasting processes of semi-solid slurry with lower solid fractions than 15%.

This work presents a new approach using a vacuum quenching mold, which is modified from the experimental apparatus previously used by Bower [8] and Martinez and Flemings [9], to evaluate the solid fraction and the particle morphology during a rheocasting process. The description of the materials, experimental setup, and experimental procedure is as follows.

The alloy used in this study was a commercial die casting alloy, Al-Si-Cu-Fe alloy (JIS ADC10), with the following chemical composition: Al = 86.44%, Si = 8.88%, Cu = 2.31%, Fe = 1.03%, Zn = 0.69%, Mn = 0.21%, Mg = 0.25%, and other minor elements = 0.19%. Approximately 2 kg of the alloy was melted in a graphite crucible. Three thermocouples were used to record the temperatures at various positions as illustrated in Figure 1. The temperature data were recorded using Winview software through a data acquisition board.

Semi-solid slurries at different solid fractions were created by the Gas Induced Semi-Solid (GISS) process [10]. In the GISS rheocasting process, a graphite diffuser is immersed into a molten metal held at a temperature a few degrees above the liquidus temperature. The cold graphite surfaces and the fine gas bubbles create a combination of local heat extraction and vigorous convection, which results in the formation of numerous solid particles.

The rapid quenching mold, shown schematically in Figure 1, consisted of two thick copper plates forming a thin channel with 1 mm thick, 30 mm wide, and 125 mm long. For some experiments, the channel thickness was adjusted to 3 mm. The copper plates were protected from the metal-mold reaction by a high temperature coating. The top end of the mold was connected to a vacuum pump with a pressure gauge and a valve. The bottom end of

the mold was covered with a small piece of thin plastic wrap, which was used to seal the vacuum within the mold. Quenched samples were obtained by lowering the copper mold, which was initially at room temperature, into the top surface of the slurry. The plastic wrap melted and evaporated instantly allowing the slurry to flow into the thin mold rapidly under the vacuum pressure. The high cooling rates achieved by the mold allowed the capture of the microstructure at a temperature, which was obtained from a thermocouple located about 1 cm underneath the melt surface at the quenching location (T3 in Figure 1).

In this study, six levels of solid fractions were obtained by varying the graphite diffuser immersion durations (rheocasting times) of 15, 17, 20, 28, 60, and 90 seconds. The channel thickness of the mold of 1 mm was used for the short rheocasting times of 15, 17, 20, and 28 seconds. Higher rheocasting times of 60 and 90 seconds yielded semi-solid slurry with the viscosity too high that the quenched samples mostly consisted of the liquid phase. Increasing the channel thickness of the mold to 3 mm was used to obtain homogeneous semi-solid quenched samples.

Metallographic examination of the quenched samples was performed at the middle location of the plate, as illustrated in Figure 2. Standard grinding and polishing processes were conduced. The samples were then etched with the Keller's reagent for about 5 seconds to reveal the rheocast solid particles. The growth layer of the particles during quenching was revealed using the Weck's reagent. The microstructure of the samples was captured using an optical microscope equipped with an image acquisition system. Brightness and contrast adjustments on the captured micrographs were carried out using Photoshop software. Image analysis was then performed on the micrographs using Image Tool software.

Representative cooling curves and the procedure to determine the slurry temperature is illustrated in Figure 3. The temperature of the semi-solid slurry at quenching was obtained

from the curves by analyzing the rheocasting times and the temperatures of the three thermocouples. For example, thermocouple 1 (T1), which was attached to the lower part of the graphite diffuser, indicated the time of immersion of 193 seconds. The time at quenching was obtained by adding the rheocasting time of 60 seconds, yielding 253 seconds. At this time on the cooling curve of T3 (thermocouple 3), the semi-solid slurry temperature was 584.5°C. Following this analysis, the slurry temperatures for different rheocasting times were acquired and summarized in Table 1.

Representative microstructures of the samples are given in Figure 4. The micrographs clearly show the solid particles of α phase formed by the rheocasting process (white particles) in the matrix of the solidified liquid phase. The number of particles increases as the rheocasting time increases, as expected. A mixture of globular and equiaxed particles are observed in the microstructures. After all the solid particles were distinguished using Photoshop and analyzed using Image Tool, the final solid fraction after quenching (f_f) was calculated using the following equation,

$$f_f = \frac{A_{pf}}{A_T} \times 100 = \frac{\sum_{i=1}^{N} A_i}{A_T} \times 100, \qquad (1)$$

where A_{pf} is the total area of the final solid particles, A_T is the total analyzed area, A_i is the final solid particle area for particle i, and N is the total number of solid particle examined.

The results of the analysis, as tabulated in Table 1, show the final solid fractions of 0.20%, 1.50%, 7.20%, 8.37%, 14.56%, and 22.10% for the rheocasting times of 15, 17, 20, 28, 60, and 90 seconds, respectively. As reported by several investigators [5-7]; however, the solid fractions obtained from quantitative metallography of quenched samples are normally higher than the true solid fractions in the slurry before quenching. The growth of the solid

particles during quenching accounts for this difference. Martinez and Flemings [9] reported that the growth layers of the solid particles could be observed by etching the samples with an appropriate etchant. By analyzing the growth layer thickness, the initial solid fraction before quenching can be obtained. In this present work, the growth layers were revealed by Weck's reagent. Representative micrographs showing the growth layers of the solid particles are given in Figure 5. The average thickness of the growth layers for each sample, $\overline{\Delta R_i}$, was analyzed by image analysis using Image Tool. The initial solid fraction of the slurry, f_0, was calculated using the analyzed data by the following equation,

$$f_0 = \frac{A_{P0}}{A_T} = \frac{\sum_{i=1}^{N}\left[\pi \cdot \left(R_i - \overline{\Delta R_i}\right)^2\right]}{A_T}, \tag{2}$$

where A_{p0} is the total area of the initial solid particles, and R_i is the radius of the solid particle i, which is calculated from the area of particle i assuming a circular shape.

The summary of the data used in the calculation and the initial solid fraction of the slurry are given in Table 2. For the rheocasting times of 15, 17, 20, 28, 60, and 90 seconds, the true solid fractions of the slurry are 0.16%, 1.13%, 5.65%, 5.99%, 12.38%, and 20.63%, respectively.

To verify the experimental data, a thermodynamic calculation using the commercial software Pandat was conducted. The Scheil model used in the calculation assumes no diffusion in the solid and a complete mixing in the liquid. For a binary alloy, the Scheil equation is given by [11],

$$f_s = 1 - \left(\frac{T_M - T}{T_M - T_L}\right)^{\frac{1}{1-k}} \tag{3}$$

where T_M is the melting point of the pure solvent, T_L is the liquidus temperature of the alloy, and k is the partition coefficient of the alloy.

The results of the calculation are plotted and compared with the experimental data in Figure 6. The final solid fraction and the initial solid fraction obtained from the experiments are slightly higher than the calculated data. This result is expected since the Scheil equation assumes no diffusion in the solid; however, with these cooling rates, there is sufficient time for solid diffusion as reported by Martinez and Flemings [9].

In summary, the experimental data obtained by this rapid quenching method combined with a correction method using the growth layer thickness are in a good agreement with the calculated data obtained by the Scheil model. The results of this work have shown that this new approach using a rapid quenching mold is an effective method to evaluate the solid fraction and the particle morphology in semi-solid slurry containing low solid fractions of an aluminum die casting alloy. The solid fraction curve in the low solid fraction range of other interested alloys can also be evaluated using this approach. In addition, this approach can be used to study the microstructure evolution of other semi-solid rheocasting processes.

This work was funded by the Thai Research Fund contract number MRG4980110. The authors would also like to thank Assoc. Prof. Lek Sikong for the guidance and support, Ms. Buasaeng, Ms. Chalinda, and the IMT team for helping with the experiments and data analysis. The permission to use a trial version of Pandat by CompuTherm LLC is gratefully acknowledged.

[1] A.M. de Figueredo, Ed. Science and Technology of Semi-Solid Metal Processing, NADCA, 2001.

[2] C.P. Hong, J.M. Kim. Solid State Phenomena. 116-117 (2006) 44-53.

[3] H. Gua, X. Yang. Solid State Phenomena. 116-117 (2006) 425-428.

[4] J. Wannasin, S. Junudom, T. Rattanochaikul, M.C. Flemings. Accepted for publication in Solid State Phenomena (2008).

[5] E. Tzimas, A. Zavaliangos, J. Mater. Sci. 35 (2000) 5319-5329.

[6] A.M. de Figueredo, Y. Sumartha, M.C. Flemings. Light Metals (1998). San Antonio, Texas, USA; 15-19 Feb. 1998. pp. 1103-106.

[7] S.-W. Chen, C.-C. Haung, Acta Mater. 44 (1996) 1955-1965.

[8] T.F. Bower, M.C. Flemings. Transactions of the Metallurgical Society of AIME, (239), February, 1967, pp. 216-219.

[9] R.A. Martinez, M.C. Flemings. Metall. Mater. Trans. 36A (2005) 2205-2210.

[10] J. Wannasin, R.A. Martinez, M.C. Flemings. Scripta Mater. 55 (2006) 115-118.

[11] M.C. Flemings. Solidification Processing. New York: McGraw-Hill Book Company, 1974.

List of Figures

List of Tables

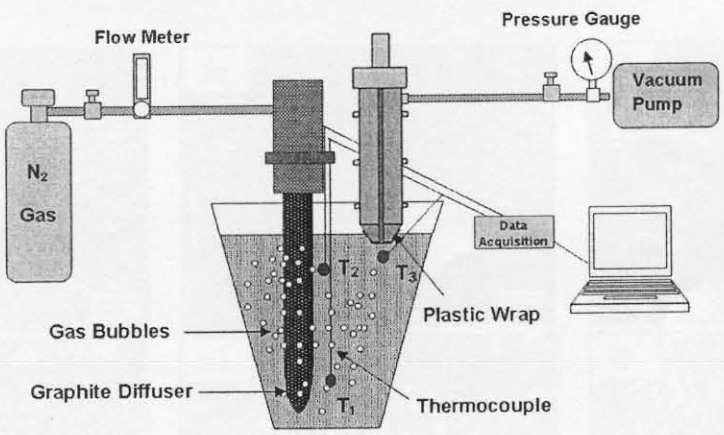

Figure 1. Schematic of experimental setup.

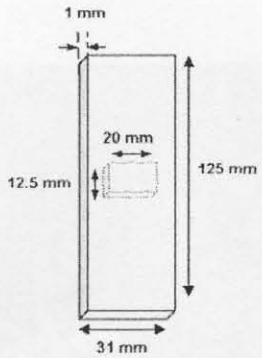

Figure 2. Quenched plate and sample location.

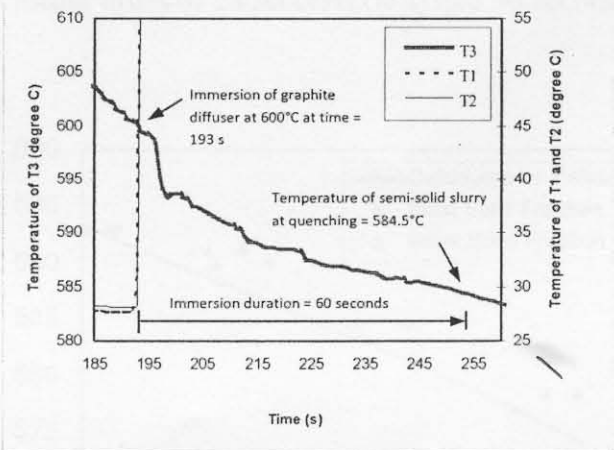

Figure 3. Representative cooling curves and the procedure to determine the slurry temperature.

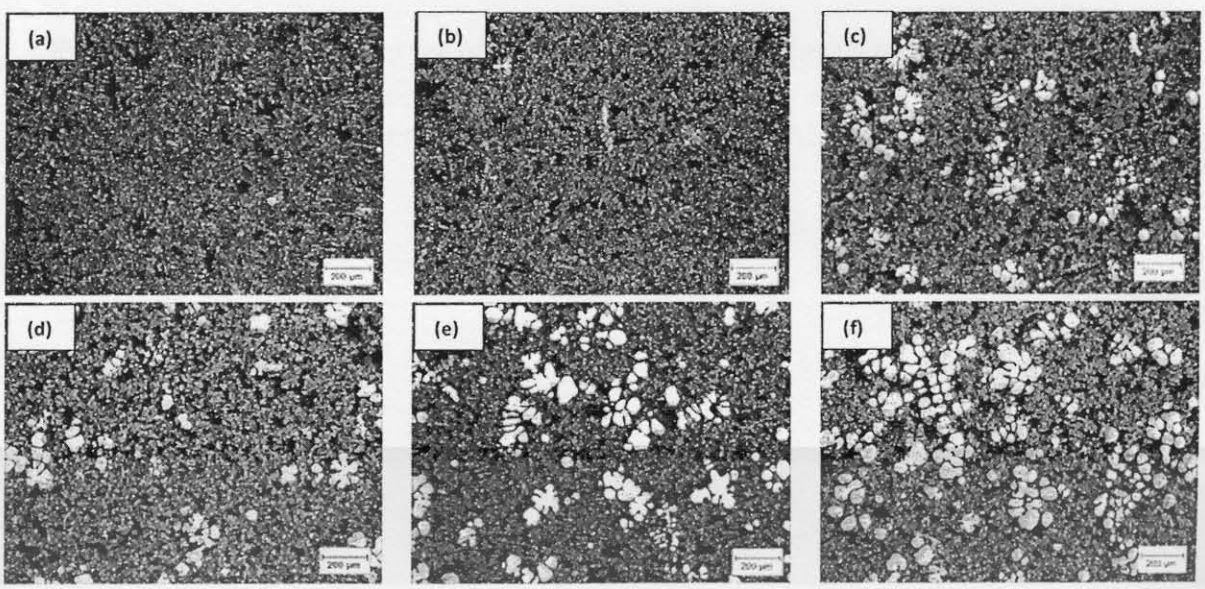

Figure 4. Representative microstructure of the samples quenched after the rheocasting times of (a) 15 s, (b) 17 s, (c) 20 s, (d) 28 s, (e) 60 s, and (f) 90 s.

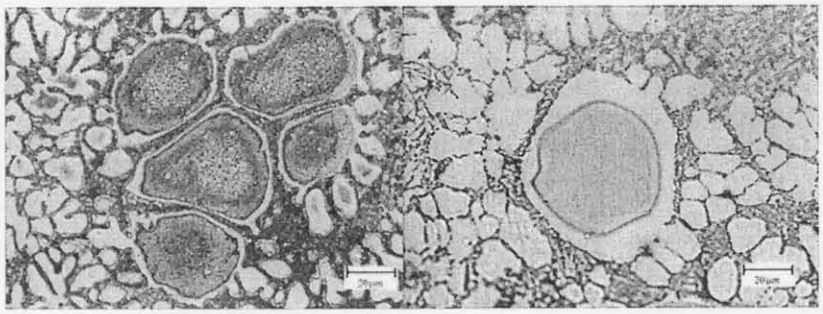

Figure 5. Representative micrographs showing the growth layer of the solid particles after the rheocasting times of 28 seconds (left) and 90 seconds (right).

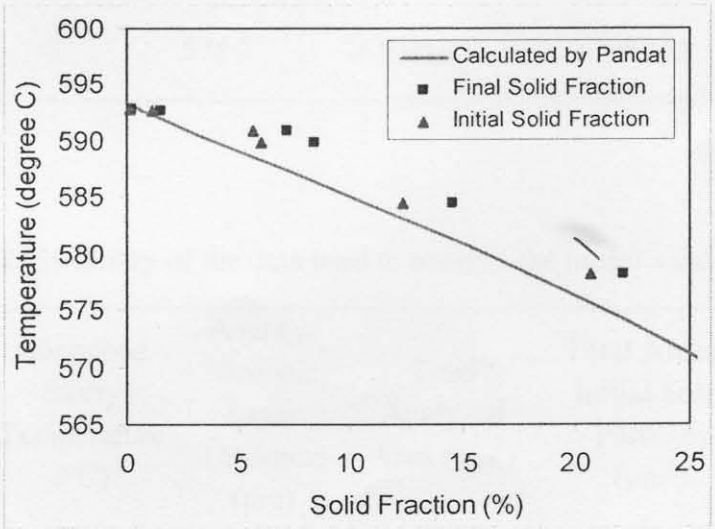

Figure 6. Solid fraction curves of the final solid fraction (analyzed from the solidified microstructure),the initial solid fraction (analyzed from the solidified microstructure and corrected by the growth layer during quenching), and the calculated data from the Scheil model.

Table 1. Summary of the data used to analyze the final solid fraction

Rheocasting Time (s)	Sample Thickness (mm)	Quenched Slurry Temperature (°C)	Total Analyzed Area (μm^2)	Total Area of Final Solid Particles (μm^2)	Final Solid Fraction (%)
15	1	592.8	26204160	53475	0.20
17	1	592.7	26204160	393462	1.50
20	1	590.9	30571520	2201211	7.20
28	1	589.9	30571520	2558166	8.37
60	3	584.5	26204160	3815031	14.56
90	3	578.2	26204160	5790240	22.10

Table 2. Summary of the data used to analyze the initial solid fraction

Rheocasting Time (s)	Quenched Slurry Temperature (°C)	Average Growth Layer Thickness (μm)	Total Analyzed Area (μm^2)	Total Area of Initial Solid Particles (μm^2)	Initial Solid Fraction (%)
15	592.8	1.7	26204160	41367	0.16
17	592.7	1.6	26204160	295659	1.13
20	590.9	2.0	30571520	1727178	5.65
28	589.9	3.6	30571520	1830212	5.99
60	584.5	3.3	26204160	3243361	12.38
90	578.2	2.7	26204160	5405998	20.63